Impact of long-term erosion on crustal stresses and seismicity in stable continental regions

Stephane Mazzotti, Xavier Vergeron, Oswald Malcles, Juliette Grosset, Philippe Vernant

GEOLOGY | THE GEOLOGICAL SOCIETY OF AMERICA®

https://doi.org/10.1130/G51327.1

Manuscript received 28 November 2022
Revised manuscript received 22 April 2023
Manuscript accepted 19 May 2023

Published online 31 May 2023

Impact of long-term erosion on crustal stresses and seismicity in stable continental regions

Stephane Mazzotti*, Xavier Vergeron, Oswald Malcles, Juliette Grosset, and Philippe Vernant
Géosciences Montpellier, Université de Montpellier, CNRS, Place Eugène Bataillon, 34095 Montpellier, France

ABSTRACT

The causes of seismicity in stable continental regions (SCRs) remain an open question, in particular with respect to (1) the transient or steady-state nature of the forcing mechanisms and (2) the bias toward shallow seismicity. In this study, we test the impact of long-term localized erosion on crustal stresses and the promotion or inhibition of seismicity in SCRs. We subject numerical models with various geotherms and rheologies to typical SCR erosion rates (4–200 m/m.y.) over 10 m.y. to estimate the lithosphere mechanical response and the associated stress perturbations. In all models, the lithosphere deformation and stresses due to long-term localized erosion are close, but not identical, to those predicted by a simple elastic plate model. In specific cases with relatively high geotherm or weak crust, upper mantle or lower crust viscous flow can significantly impact the upper crust stress perturbations. Overall, erosion-induced horizontal tension is maximum in the upper crust (0–10 km depth) and much smaller in the mid- and lower crust. These stress perturbations reach a few tens of megapascals to a few megapascals over a few million years. Depending on the erosion patterns and regional state of stress, they can promote fault instability and seismicity for all faulting styles. Our results suggest that erosion-induced stresses can contribute to explaining the bias toward shallow seismicity in SCRs.

INTRODUCTION

The origin of seismicity in stable continental regions (SCRs) is an old scientific conundrum (Sykes, 1978; Johnston and Kanter, 1990) (hereafter, SCRs refer to continental regions far from active plate boundaries, with very limited recent tectonic activity; e.g., Australia, central-eastern North America). A variety of processes are proposed to explain SCR seismicity: from mantle dynamics or lithosphere heterogeneities acting on geological time scales, to glacial isostatic adjustment or erosion pulses on thousand-year time scales (Mazzotti, 2007; Calais et al., 2010; Ghosh et al., 2019). This uncertainty in the steady-state or transient nature of the forcing mechanisms results in ongoing debates on the spatial and temporal distribution, clustering, and recurrence of large SCR earthquakes (Clark et al., 2012; Page and Hough, 2014; Calais et al., 2016). Another peculiarity is that large SCR ruptures appear biased to shallow (0–10 km) depths (Klose and Seeber, 2007; Jackson and McKenzie, 2022). This lack of understanding on the origin of SCR earthquakes results in strong uncertainties in the characterization of seismic hazard, with significant implications for populations or critical infrastructures (Stein and Mazzotti, 2007).

In this study, we assess the impact of long-term localized erosion (acting on millions of years) on crustal stresses and its potential role as a forcing or promoting mechanism of SCR seismicity. Although long-term erosion is identified as a key process in the evolution of topography and tectonics (Vernant et al., 2013; Braun et al., 2014), its impact on SCR deformation and seismicity has been little studied (e.g., Eastern Tennessee seismic zone, central-eastern USA; Gallen and Thigpen, 2018). Here, we propose a simple conceptual model that relates long-term erosion, induced crustal stresses, and promotion or inhibition of seismicity in different SCR systems.

The response of the lithosphere to long-term erosion is commonly assumed to follow the mechanical behavior of an elastic plate overlying a low-viscosity fluid (Champagnac et al., 2007; Gallen and Thigpen, 2018). This model predicts specific stress patterns that strongly depend on the assumed, commonly poorly constrained, elastic plate thickness (e.g., lateral and vertical transitions between horizontal tension or compression domains). In order to assess the impact of long-term erosion on crustal stresses and seismicity without assuming a specific type of mechanical behavior, we use finite-element models to test various erosion rates on a pre-stressed lithosphere represented by standard crustal and mantle rheologies. Our models cover the range of lithosphere rigidities estimated in SCRs, from weak passive margins to the strong cratons.

MODELS AND PARAMETERS

The lithosphere is represented by elasto-visco-plastic rheologies (Table S1 in the Supplemental Material[1]), with a 40-km-thick quartz or diabase crust over an olivine upper mantle, underlain by a hydrostatic restoration boundary condition (Fig. 1). A uniform geotherm is applied over the whole model, with three cases defined by the Moho temperature = 500, 600, and 800 °C and the base of the thermal lithosphere = 150, 100, and 70 km. These six combinations (three geotherms × two crust compositions) represent a large panel of lithospheric strength profiles. The models are subjected for 10 m.y. to a constant, uniform, localized erosion rate over a 100-km-long area (see the Supplemental Material). Tested erosion rates are representative of the range of regional average erosion rates (~4–200 m/m.y.) in SCRs over 10 ka–10 Ma (Portenga and Bierman, 2011; Beauvais and Chardon, 2013; Harel et al., 2016).

Before applying erosion, the models are pre-stressed by application of an inward velocity of 0.5 mm/a (Fig. 1; cf. Tarayoun et al., 2019). This

Stephane Mazzotti https://orcid.org/0000-0003-2514-4310
*stephane.mazzotti@umontpellier.fr

[1]Supplemental Material. Model setup, yield stress classes, lithosphere mechanical response, fault stability margin, and earthquake depths. Please visit https://doi.org/10.1130/GEOL.S.23063186 to access the supplemental material, and contact editing@geosociety.org with any questions.

CITATION: Mazzotti, S., et al., 2023, Impact of long-term erosion on crustal stresses and seismicity in stable continental regions: Geology, v. 51, p. 733–737, https://doi.org/10.1130/G51327.1

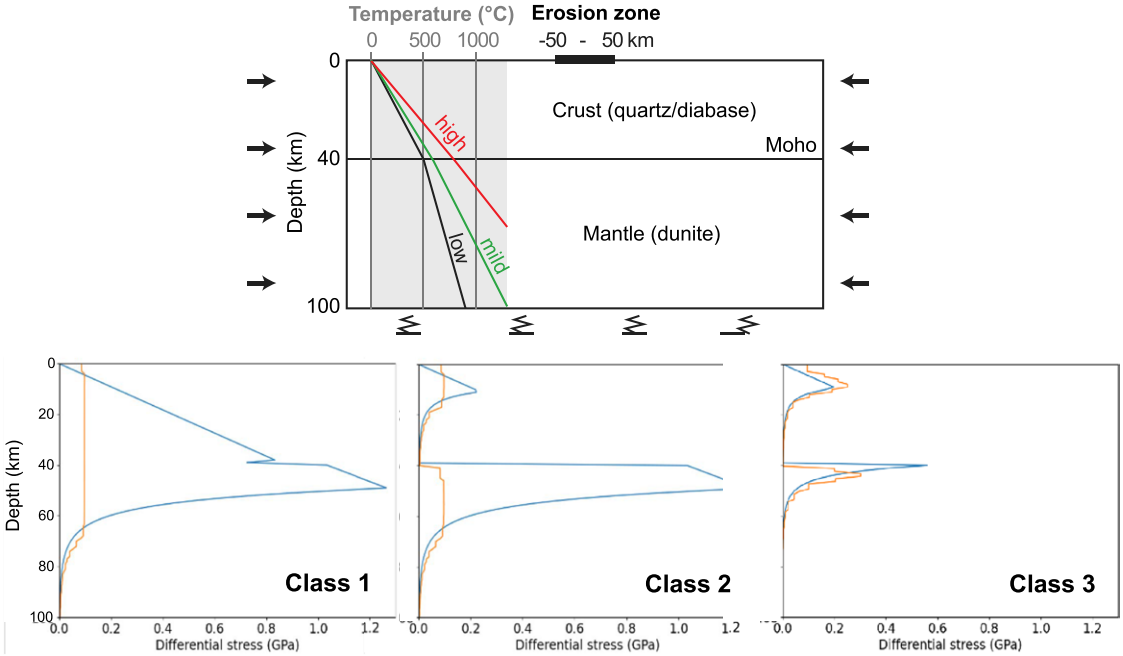

Figure 1. Model setup and classes. Top: Setup with three geotherms (high, mild, low) and two crustal rheologies (quartz, diabase). Model boundary conditions shown by lateral arrows (shortening rate) and bottom symbols (hydrostatic restoration). Bottom: Differential stress profiles for class 1, 2, and 3 models. Blue curves are theoretical brittle-ductile yield stress profiles defined by geotherms and rheology laws; orange curves are force-limited stress profiles used in our models (see Models and Parameters section in text).

initial stage is continued until the whole model reaches differential stresses such that the lithosphere integrated strength is at equilibrium with a standard tectonic resultant force of 1–10 × 10^{12} N/m (Reynolds et al., 2002; Copley et al., 2010; Tarayoun et al., 2019). This results in differential stress profiles ranging from fully brittle or ductile (hot geotherm–weak crust models) to cases where an elastic core remains in the crust or the mantle (cold geotherm–strong crust models) (Fig. 1; Fig. S1 in the Supplemental Material). These latter types are meant to represent a strong, cold, slowly deforming lithosphere characteristic of SCRs with high flexural rigidity (Hyndman et al., 2009; Tesauro et al., 2012) without having to assume elastic stress thresholds or profiles.

The resulting models are categorized in three classes (Fig. 1; Fig. S1): class 1—models with one elastic core either only in the crust or in the crust and upper mantle; class 2—models with two elastic cores in the upper crust and the upper mantle, separated by a ductile lower crust; and class 3—models with fully brittle or ductile crust and mantle.

LITHOSPHERE MECHANICAL RESPONSE

In all models, the mechanical response of the lithosphere to long-term erosion rates shows similarities with that of an elastic plate, including upward bending and associated bending stresses (surface tension–basal compression) below and on the side of the region of erosion (Figs. S2–S8). The equivalent elastic-plate thickness (noted T_e) that best fits the peak uplift below the erosion zone depends on both erosion rates and durations: slower rates and shorter durations are associated with higher T_e. In detail, three main types of responses can be defined (Fig. 2):

- Deformation and stresses are well represented by the flexure of an elastic plate of thickness similar to that of the model elastic core (Figs. 2A and 2D). This is also shown by the presence of a subsidence bulge outside of the erosion region with the associated downward bending stresses (surface compression–basal tension). This corresponds to models with elastic cores in both mantle and crust (cf. Fig. 1, class 1).
- The model response deviates from elastic flexure due to viscous relaxation in the upper mantle, which results in more concentrated deformation, a narrowed uplift zone, and higher stresses at depth (compared to an elastic plate; Figs. 2B and 2E). This corresponds to models with limited uppermost mantle resistance, either elastic or plastic.
- The model shows large deviations from elastic flexure due to viscous relaxation in both upper mantle and lower crust. In these cases, lower crustal flow results in a lack of subsidence bulge outside of the erosion region and small bending stresses limited to the upper crust (Figs. 2C and 2F).

These types correspond to three end members (purely elastic, viscous mantle, viscous lower crust), with some models evolving between them depending on the viscous resistance of the upper mantle and lower crust controlled by erosion rates and durations. For example, class 1 models with an elastic core limited to the crust show a transition from the second type to the first type with increasing erosion rates and durations due to the non-Newtonian viscosity laws: a slow erosion rate and short duration result in high effective viscosity and significant viscous resistance in the upper mantle, which impacts the crustal response, whereas a faster erosion rate or longer duration result in lower effective viscosity, a fully relaxed mantle, and a lithospheric response limited to the crust.

EROSION-INDUCED CRUSTAL STRESSES AND POTENTIAL EARTHQUAKE PROMOTION

Figure 3 illustrates the horizontal stress induced by 40 and 100 m/m.y. erosion rates after 2 m.y.: horizontal tension is limited to the upper crust and maximum between 0 and 10 km, and mid- and lower crust stresses are small, except for compressive stress in a few models (e.g., lower crustal flow). The seismogenic impact of these stress perturbations can be assessed using the fault stability margin (FSM) indicator based on the Mohr-Coulomb failure criterion (Wu and Hasegawa, 1996; Fig. S8):

$$\mathrm{FSM} = C\cos\phi + \frac{1}{2}(\sigma_1+\sigma_3)\sin\phi - \frac{1}{2}(\sigma_1-\sigma_3), \quad (1)$$

with σ_1 and σ_3 the maximum and minimum principal stresses acting on a fault, respectively, and C and ϕ the fault cohesion and friction angle, respectively. Relative to a reference pre-erosion state of stress, the variation of FSM due to erosion is:

$$d\mathrm{FSM} = \frac{1}{2}(d\sigma_1+d\sigma_3)\sin\phi - \frac{1}{2}(d\sigma_1-d\sigma_3), \quad (2)$$

with $d\sigma_1$ and $d\sigma_3$ the variations of σ_1 and σ_3 due to erosion. Hereafter, these principal stress perturbations are based on the erosion-induced stresses expressed as σ_H, σ_h, and σ_V, the maxi-

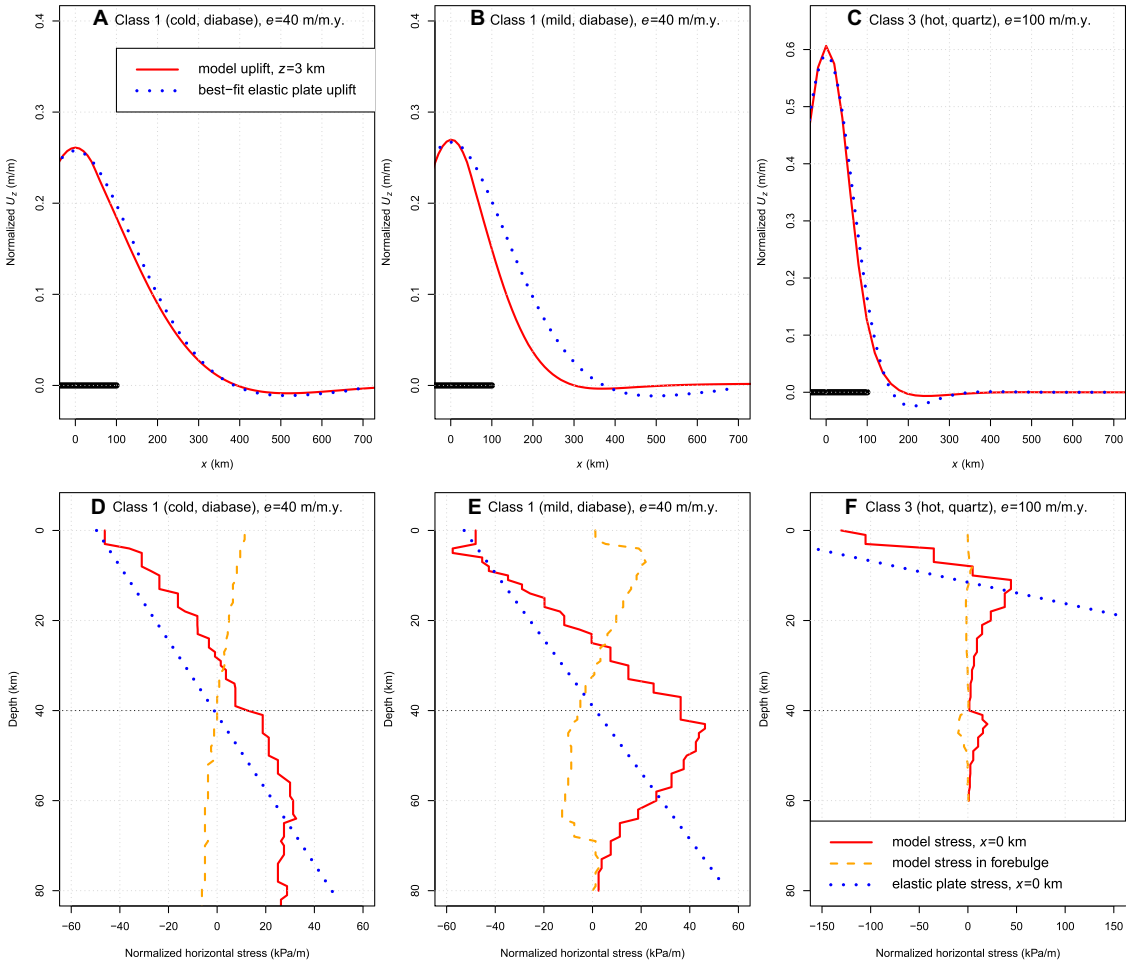

Figure 2. Erosion-induced uplift and horizontal stress at 2 m.y. model time. Uplift and stress are normalized by amount of erosion. (A–C) Surface uplift (*Uz*) for models and best-fit elastic plates. Thick black lines show erosion zone. (D–F) Depth distribution of model horizontal stress at center of erosion (*x* = 0 km) and in lateral bulge (*x* = 300–600 km) versus elastic plate stress at center of erosion. Cold, mild, and hot describe model geotherms; diabase and quartz describe model crust rheology. *e*—erosion rate (see text).

mum horizontal, minimum horizontal, and vertical stresses, respectively.

The impact on fault activity and seismicity depends on (1) the geometric relationship between the initial state of stress and the perturbations and (2) the regional faulting style. The simplest case corresponds to a spatially homogeneous erosion pattern in which erosion rates are approximately constant in all directions over a few hundred kilometers (hereafter, stress values are normalized by the amount of erosion to facilitate comparisons). In this case, erosion produces near-isotropic horizontal tension ($\sigma_H \approx \sigma_h$) of ~−20 to −60 kPa/m in the upper crust (Fig. 3). The vertical stress σ_V due to overburden removal is ~−25 kPa/m. Assuming Andersonian regimes for optimally oriented faults and $\phi = 30°$, the *d*FSM for reverse, strike-slip, and normal faulting styles are ~−10, −20, and −25 kPa/m, respectively. Thus, a homogeneous erosion pattern brings all types of faulting closer to failure (Fig. S8), with negative *d*FSM reaching a few megapascals for slow erosion rates over a few million years (e.g., for reverse faulting and 20 m/m.y. erosion rate over 5 m.y., *d*FSM ≈ −1 MPa). Such stress perturbations of a few tenths to a few megapascals are small compared to the state of stress in the crust, but they are sufficient to promote fault instability and advance the occurrence of earthquakes on pre-stressed, near-failure faults (Gomberg et al., 1998; Stein, 1999). Thus, slow erosion rates may promote seismicity in low-relief SCRs such as Australia or central North America. More specifically, it may contribute to explaining the bias toward shallow seismicity in these SCRs, where 80% of the seismic moment release occurs above 7 km depth and the mid-crust is mostly aseismic (Fig. 3) (Klose and Seeber, 2007; Jackson and McKenzie, 2022).

Other cases with more complex erosion patterns require specific analyses of the interactions between the regional state of stress, faulting styles, and the effect of anisotropic stress perturbations. A specific example can be derived for an erosion pattern with high erosion rates along an elongated region surrounded by low rates. Such a case can apply to SCRs where relict topography from old orogens forms an elongated zone of higher relief susceptible to higher erosion rates relative to the surrounding platforms (e.g., Appalachian Mountains, USA; Ural Mountains, Russia; Eastern Highlands, Australia). Within the high-topography area, erosion-induced horizontal tension (σ_H) is perpendicular to the elongated topography axis, whereas the topography-parallel stress perturbation (σ_h) is null. The interaction with the regional stress field promotes seismicity (negative *d*FSM) for all faulting styles if the regional σ_H is subparallel to the topography long axis. This case may apply to the seismic zones of the eastern Tennessee mountains, USA, or the Armorican Massif, France. At the opposite end, if the regional σ_H is orthogonal to the topography long axis, the erosion-induced horizontal tension would only promote reverse faulting while inhibiting strike-slip and normal faulting styles.

DISCUSSION

Our models indicate that in many cases, long-term localized erosion can promote fault instability and seismicity for all faulting styles in SCRs. After a few million years, slow erosion rates result in stress perturbations of a few tenths to a few megapascals. Because these are not large enough to overcome a regional stress field, faulting and seismicity can be promoted (or in some cases inhibited) by local erosion but remain controlled by other processes. Our results also highlight the importance of dedicated studies to account for the variabilities and uncertainties in erosion rates and in the lithosphere mechanical state. Examples of specific

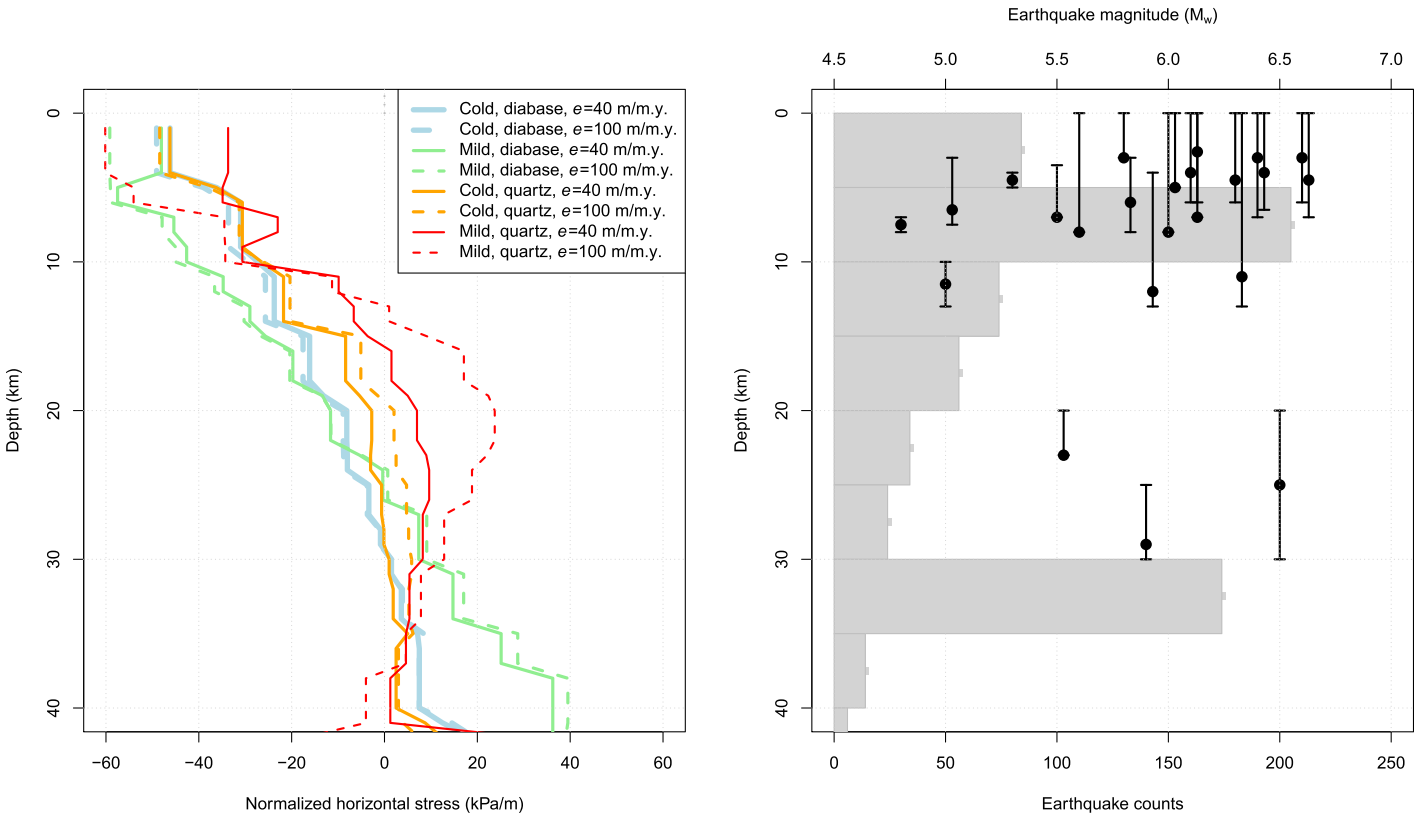

Figure 3. Erosion-induced crustal stress and stable continental region (SCR) seismicity depth distribution. Left: Horizontal stress perturbations at 2 m.y. model time normalized by amount of erosion. Cold and mild describe model geotherms; diabase and quartz describe model crust rheology. *e*—erosion rate (see text). Right: Seismicity depth distribution. Black dots and bars show epicenters and rupture extents of $M_w \geq 5.0$ SCR earthquakes (after Klose and Seeber, 2007; Table S2 [see text footnote 1]). Gray bars are a histogram of SCR earthquake depths (global catalog of Schulte and Mooney, 2005; see Supplemental Material).

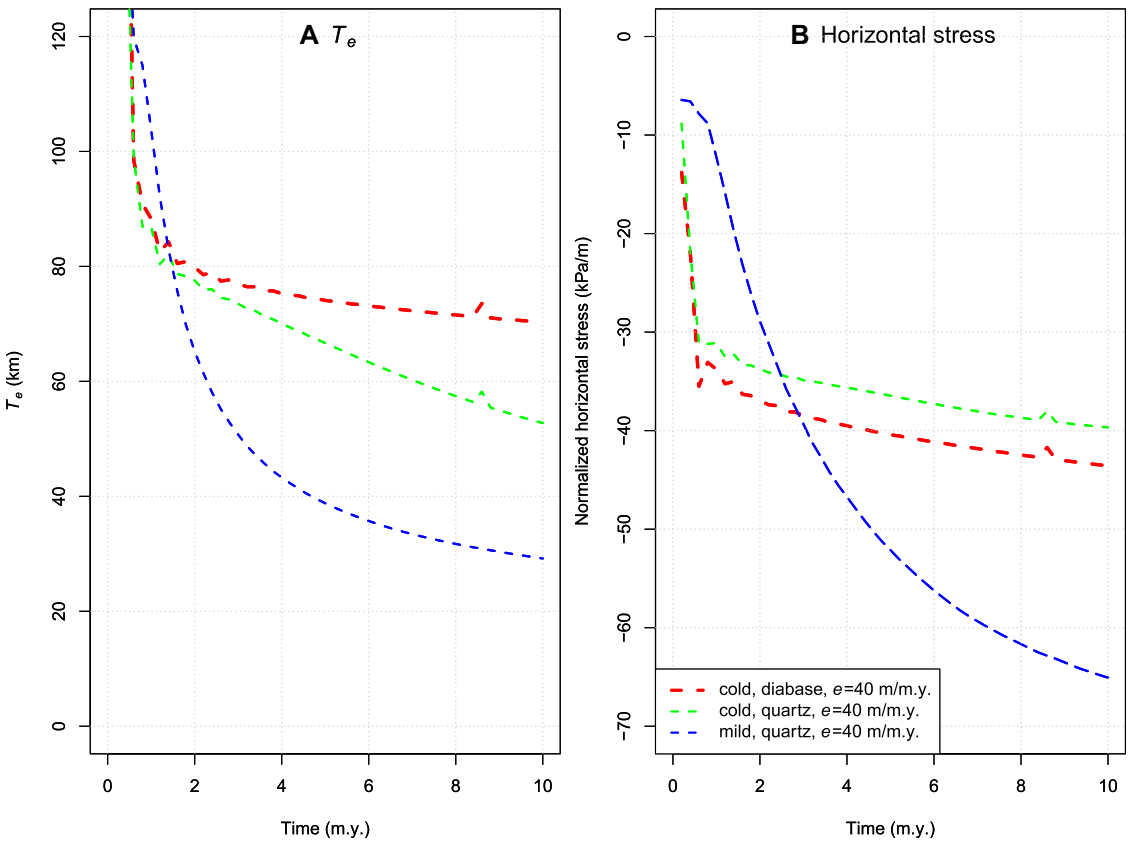

Figure 4. Time dependence of mechanical response to erosion. (A) Equivalent elastic-plate thickness (*Te*) (based on peak uplift below erosion). (B) Horizontal stress averaged between 2 and 8 km depth. Cold and mild describe model geotherms; diabase and quartz describe model crust rheology. *e*—erosion rate (see text).

erosion rate variations include drainage divide migration or capture that can significantly impact local erosion on million-year time scales (Sassolas-Serrayet et al., 2019).

Our range of model strengths (Fig. 1) is representative of the variability in lithosphere rigidity derived from rheological and inverse methods (Tesauro et al., 2012), with T_e varying from 20–30 km (e.g., eastern Australian margin) to >100 km (e.g., North America craton). In the latter cases, the impact of long-term erosion can be modeled using a simple elastic plate approach. In contrast, SCRs with low T_e, mild or hot geotherms, or weak crust (e.g., central-western Europe) require specific attention due to potential upper mantle or lower crust viscous relaxation. In these cases, the lithosphere response deviates from that of an elastic plate, precluding simple inferences on the amplitude and depth distribution of erosion-induced stresses or the effect of an inexistant lateral bulge (Figs. 2C and 2F). An additional complexity requiring further analyses is the effect of structural inheritance on lateral variation and anisotropy in lithosphere resistance and its mechanical response to external forcing (Tarayoun et al., 2019).

The temporal dependance of the lithosphere response to long-term localized erosion also requires further consideration. As shown in Figure 4, two main phases are identified: an initial phase of strong T_e decrease and stress increase in the first 1–2 m.y., followed by a second phase of slower variation. This is due to the nonlinear strain-rate-dependent viscous flow laws, in particular for models with significant lower crustal flow, which results in strong temporal variations and T_e decrease and stress increase by a factor of ~2 between 2 and 10 m.y. (Fig. 4). A similar time dependence of T_e to viscoelastic relaxation has been proposed in previous studies (Watts et al., 2013). This points out the difficulty of choosing a "correct" elastic thickness when modeling the response to surface loads and forcing, such as erosion rates.

ACKNOWLEDGMENTS

This study was supported by the French Agence Nationale de la Recherche, project ANR-20-CE01-0005 "EroSeis." Models, data analyses, and figures are done with open-source, free software (https://code.google.com/archive/p/adeli/; https://www.python.org/; https://www.r-project.org/; https://www.paraview.org/). Model parameters and results are available on demand on the Open Science Framework, "EroSeis" project (https://osf.io/yq3bt/). We thank Sean Gallen and two anonymous reviewers for their constructive reviews.

REFERENCES CITED

Beauvais, A., and Chardon, D., 2013, Modes, tempo, and spatial variability of Cenozoic cratonic denudation: The West African example: Geochemistry, Geophysics, Geosystems, v. 14, p. 1590–1608, https://doi.org/10.1002/ggge.20093.

Braun, J., Simon-Labric, T., Murray, K.E., and Reiners, P.W., 2014, Topographic relief driven by variations in surface rock density: Nature Geoscience, v. 7, p. 534–540, https://doi.org/10.1038/ngeo2171.

Calais, E., Freed, A.M., Van Arsdale, R., and Stein, S., 2010, Triggering of New Madrid seismicity by late-Pleistocene erosion: Nature, v. 466, p. 608–611, https://doi.org/10.1038/nature09258.

Calais, E., Camelbeeck, T., Stein, S., Liu, M., and Craig, T.J., 2016, A new paradigm for large earthquakes in stable continental plate interiors: Geophysical Research Letters, v. 43, p. 10,621–10,637, https://doi.org/10.1002/2016GL070815.

Champagnac, J.D., Molnar, P., Anderson, R.S., Sue, C., and Delacou, B., 2007, Quaternary erosion-induced isostatic rebound in the western Alps: Geology, v. 35, p. 195–198, https://doi.org/10.1130/G23053A.1.

Clark, D., McPherson, A., and Van Dissen, R., 2012, Long-term behaviour of Australian stable continental region (SCR) faults: Tectonophysics, v. 566–567, p. 1–30, https://doi.org/10.1016/j.tecto.2012.07.004.

Copley, A., Avouac, J.-P., and Royer, J.-Y., 2010, India-Asia collision and the Cenozoic slowdown of the Indian plate: Implications for the forces driving plate motions: Journal of Geophysical Research, v. 115, B03410, https://doi.org/10.1029/2009JB006634.

Gallen, S.F., and Thigpen, J.R., 2018, Lithologic controls on focused erosion and intraplate earthquakes in the eastern Tennessee seismic zone: Geophysical Research Letters, v. 45, p. 9569–9578, https://doi.org/10.1029/2018GL079157.

Ghosh, A., Holt, W.E., and Bahadori, A., 2019, Role of large-scale tectonic forces in intraplate earthquakes of central and eastern North America: Geochemistry, Geophysics, Geosystems, v. 20, p. 2134–2156, https://doi.org/10.1029/2018GC008060.

Gomberg, J., Beeler, N.M., Blanpied, M.L., and Bodin, P., 1998, Earthquake triggering by transient and static deformations: Journal of Geophysical Research, v. 103, p. 24,411–24,426, https://doi.org/10.1029/98JB01125.

Harel, M.-A., Mudd, S.M., and Attal, M., 2016, Global analysis of the stream power law parameters based on worldwide ^{10}Be denudation rates: Geomorphology, v. 268, p. 184–196, https://doi.org/10.1016/j.geomorph.2016.05.035.

Hyndman, R.D., Currie, C.A., Mazzotti, S., and Frederiksen, A., 2009, Temperature control of continental lithosphere elastic thickness, *Te* vs *Vs*: Earth and Planetary Science Letters, v. 277, p. 539–548, https://doi.org/10.1016/j.epsl.2008.11.023.

Jackson, J., and McKenzie, D., 2022, The exfoliation of cratonic Australia in earthquakes: Earth and Planetary Science Letters, v. 578, 117305, https://doi.org/10.1016/j.epsl.2021.117305.

Johnston, A.C., and Kanter, L.R., 1990, Earthquakes in stable continental crust: Scientific American, v. 262, p. 68–75, https://doi.org/10.1038/scientificamerican0390-68.

Klose, C.D., and Seeber, L., 2007, Shallow seismicity in stable continental regions: Seismological Research Letters, v. 78, p. 554–562, https://doi.org/10.1785/gssrl.78.5.554.

Mazzotti, S., 2007, Geodynamic models for earthquake studies in intraplate North America, *in* Stein, S., and Mazzotti, S., eds., Continental Intraplate Earthquakes: Science, Hazard, and Policy Issues: Geological Society of America Special Paper 425, p. 17–33, https://doi.org/10.1130/2007.2425(02).

Page, M.T., and Hough, S.E., 2014, The New Madrid Seismic Zone: Not dead yet: Science, v. 343, p. 762–764, https://doi.org/10.1126/science.1248215.

Portenga, E.W., and Bierman, P.R., 2011, Understanding Earth's eroding surface with ^{10}Be: GSA Today, v. 21, no. 8, p. 4–10, https://doi.org/10.1130/G111A.1.

Reynolds, S.D., Coblentz, D.D., and Hillis, R.R., 2002, Tectonic forces controlling the regional intraplate stress field in continental Australia: Results from new finite element modeling: Journal of Geophysical Research, v. 107, p. ETG 1-1–ETG 1-15, https://doi.org/10.1029/2001JB000408.

Sassolas-Serrayet, T., Cattin, R., Ferry, M., Godard, V., and Simoes, M., 2019, Estimating the disequilibrium in denudation rates due to divide migration at the scale of river basins: Earth Surface Dynamics, v. 7, p. 1041–1057, https://doi.org/10.5194/esurf-7-1041-2019.

Schulte, S.M., and Mooney, W.D., 2005, An updated global earthquake catalogue for stable continental regions: Reassessing the correlation with ancient rifts: Geophysical Journal International, v. 161, p. 707–721, https://doi.org/10.1111/j.1365-246X.2005.02554.x.

Stein, R.S., 1999, The role of stress transfer in earthquake occurrence: Nature, v. 402, p. 605–609, https://doi.org/10.1038/45144.

Stein, S., and Mazzotti, S., eds., 2007, Continental Intraplate Earthquakes: Science, Hazard, and Policy Issues: Geological Society of America Special Paper 425, 402 p., https://doi.org/10.1130/978-0-8137-2425-6.

Sykes, L.R., 1978, Intraplate seismicity, reactivation of preexisting zones of weakness, alkaline magmatism, and other tectonism postdating continental fragmentation: Reviews of Geophysics, v. 16, p. 621–688, https://doi.org/10.1029/RG016i004p00621.

Tarayoun, A., Mazzotti, S., and Gueydan, F., 2019, Quantitative impact of structural inheritance on present-day deformation and seismicity concentration in intraplate deformation zones: Earth and Planetary Science Letters, v. 518, p. 160–171, https://doi.org/10.1016/j.epsl.2019.04.043.

Tesauro, M., Audet, P., Kaban, M.K., Bürgmann, R., and Cloetingh, S., 2012, The effective elastic thickness of the continental lithosphere: Comparison between rheological and inverse approaches: Geochemistry, Geophysics, Geosystems, v. 13, Q09001, https://doi.org/10.1029/2012GC004162.

Vernant, P., Hivert, F., Chéry, J., Steer, P., Cattin, R., and Rigo, A., 2013, Erosion-induced isostatic rebound triggers extension in low convergent mountain ranges: Geology, v. 41, p. 467–470, https://doi.org/10.1130/G33942.1.

Watts, A.B., Zhong, S.J., and Hunter, J., 2013, The behavior of the lithosphere on seismic to geologic timescales: Annual Review of Earth and Planetary Sciences, v. 41, p. 443–468, https://doi.org/10.1146/annurev-earth-042711-105457.

Wu, P., and Hasegawa, H.S., 1996, Induced stresses and fault potential in eastern Canada due to a disc load: A preliminary analysis: Geophysical Journal International, v. 125, p. 415–430, https://doi.org/10.1111/j.1365-246X.1996.tb00008.x.

Printed in USA